

# Investigation of Self-Injection Locked Visible Laser Diodes for High Bit-Rate Visible Light Communication

Volume 10, Number 4, August 2018

Md Hosne Mobarok Shamim

Mohamed Adel Shemis

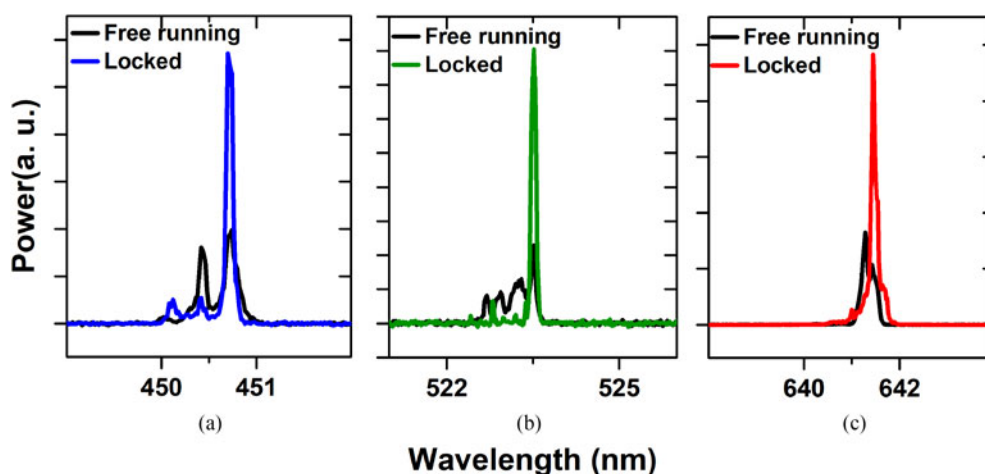
Chao Shen

Hassan M. Oubei

Tien Khee Ng, *Senior Member, IEEE*

Boon S. Ooi, *Senior Member, IEEE*




Mohammed Zahed Mustafa Khan, *Senior Member, IEEE*



DOI: 10.1109/JPHOT.2018.2849884

1943-0655 © 2018 IEEE

# Investigation of Self-Injection Locked Visible Laser Diodes for High Bit-Rate Visible Light Communication

Md Hosne Mobarok Shamim <sup>1</sup>, Mohamed Adel Shemis,<sup>1</sup>  
Chao Shen,<sup>2</sup> Hassan M. Oubei <sup>2</sup>,  
Tien Khee Ng <sup>2</sup>, *Senior Member, IEEE*,  
Boon S. Ooi <sup>2</sup>, *Senior Member, IEEE*,  
and Mohammed Zahed Mustafa Khan <sup>1</sup>, *Senior Member, IEEE*

<sup>1</sup>Optoelectronics Research Laboratory, Electrical Engineering Department, King Fahd University of Petroleum & Minerals, Dhahran 31261, Saudi Arabia

<sup>2</sup>Photonics Laboratory, Computer, Electrical, and Mathematical Sciences and Engineering Division, King Abdullah University of Science and Technology, Thuwal 23955-6900, Saudi Arabia

DOI:10.1109/JPHOT.2018.2849884

1943-0655 © 2018 IEEE. Translations and content mining are permitted for academic research only. Personal use is also permitted, but republication/redistribution requires IEEE permission. See [http://www.ieee.org/publications\\_standards/publications/rights/index.html](http://www.ieee.org/publications_standards/publications/rights/index.html) for more information.

Manuscript received May 10, 2018; revised June 1, 2018; accepted June 19, 2018. Date of publication June 22, 2018; date of current version July 17, 2018. This work was supported in part by Deanship of Research, King Fahd University of Petroleum and Minerals under Grant KAUST004, in part by King Abdulaziz City for Science and Technology under Grants EE2381 and TIC R2-FP-008, in part by the King Abdullah University of Science and Technology (KAUST) baseline funding BAS/1/1614-01-01, KAUST funding KCR/1/2081-01-01, and GEN/1/6607-01-01, and in part by KAUST-KFUPM Special Initiative (KKI) Program REP/1/2878-01-01. Corresponding author: Mohammed Zahed Mustafa Khan (e-mail: zahedmk@kfupm.edu.sa).

**Abstract:** We report on self-injection locking in InGaN/GaN (blue/green) and InGaP/AlGaInP (red) visible-light laser diodes. The free-space optical feedback path was accomplished via an external mirror. The effect of injection current, optical power injection ratio, and external cavity length on the spectral linewidth and modulation bandwidth of the lasers is investigated. Our results show that the laser performance was substantially improved. In particular, we achieved a significant increase of ~57% (1.53–2.41 GHz) and ~31% (1.72–2.26 GHz) in the modulation bandwidth, and ~9 (1.0–0.11 nm) and ~9 (0.63–0.07 nm) times reduction in spectral linewidth of the green and blue lasers, respectively. Consequently, side-mode-suppression-ratio was considerably increased in all the cases, reaching as high as ~20 dB in self-injection locked blue laser diode, thus enabling a close to single-mode operation. This paper paves the way for attaining high-speed optical wireless communications by overcoming the challenges of limited modulation bandwidth and multimode operation of visible laser diodes with this simple scheme.

**Index Terms:** Self-injection locking, external cavity diode laser, modulation bandwidth, spectral linewidth, visible light communication.

## 1. Introduction

The internet boom at the end of the 20th century is now, in the 21st century, and expected to increase more than twice from 128 exabytes/month in 2017 to 278 exabytes/month in 2021 [1]. Thanks to today's broadband services such as, social networking, high definition video-on-demand

(HDVoD) and cloud storage and computing, that have raised the demand for high-performance and high-capacity communication technologies. Although substantial efforts are underway focusing on long-haul access networks, we are still trapped with wired/wireless microwave communication at the user end, whose network capacity is reaching saturation. To overcome this shortcoming in indoor communication, visible light has been proposed as an alternative for simultaneous illumination and optical wireless communication. This stems from several advantages offered by the visible light communication (VLC) such as energy efficiency, secure communication, no electromagnetic interferences, and more importantly unregulated spectrum.

In this regard, light emitting diodes (LED) have been identified as a viable transmitter source for VLC and illumination, with reasonably high data rates of more than 1 Gb/s using discrete multitone (DMT) modulation technique [2], [3]. However, looking at the future demand of high speed connectivity researchers have shifted their focus from the LED to the laser diodes as a possible source for illumination and communication; thanks to their higher modulation bandwidth enabling them to reach 2–18 Gb/s data transmission capacity employing direct modulation scheme such as On-Off Keying (OOK) and 16-quadrature amplitude modulation (QAM) [4]–[8]. Furthermore, optical injection locking [9] have been employed to improve the visible laser modulation bandwidth and push the boundaries of data rate beyond 10 s of Gb/s with higher order modulation schemes [10]. In literature, two types of optical injection locking have been reported, namely, external injection locking (EIL) [11] and self-injection locking (SIL) [12]. EIL employs a high-quality master laser source to inject the optical power into the slave laser to lock a single longitudinal mode from its optical spectrum, thereby enhancing the modulation bandwidth and improving the performance to that of the master laser. On the other hand, SIL employs a reflector instead of a master laser, to re-inject part of the laser light beam back into its active region, while additionally creating an external cavity. In the following, we summarize the results reported via both the assisting schemes on visible semiconductor laser diodes.

Two-stage EIL has been deployed by Lin *et al.* [13] on 680 nm red vertical cavity surface emitting laser (VCSEL), thus successfully reporting 56 Gb/s data transmission using pulse amplitude modulation (PAM4) scheme in a 20 m indoor free space channel. Subsequently, an improvement in the modulation bandwidth from 5.2 GHz to 26 GHz and then to 41.8 GHz using two and three-stage external injection-locked VCSELs were demonstrated, and with 25 and 40 Gb/s error-free data transmission, respectively, along a 50-m indoor free space channel [14]. In addition, an increase in the optical power was observed in EIL case compared to the free-running case, a signature of injection locking. Later, Lu *et al.* also explored two-stage EIL in underwater optical wireless communication (UWOC) using 16-QAM orthogonal frequency division multiplexed (OFDM) modulation scheme at 405 nm violet laser [15]. Successful demonstration of 9.6 Gb/s data transmission over 8 m underwater link was reported. In general, these works were more focused on the transmission experiments rather than investigating EIL phenomenon and the device physics on the visible laser diodes.

Very recently, owing to the merits offered by SIL *viz.* energy efficiency, compact scheme, etc., our group successfully demonstrated SIL on 524 nm green [16] and 450 nm blue InGaN/GaN diode lasers [17]. Besides, [18] utilized SIL to demonstrate a single longitudinal mode operation at 446.5 nm blue laser diode with magnesium fluoride ( $\text{MgF}_2$ ) whispering gallery mode (WGM) resonator. In this work, for the first time to our knowledge, we comprehensively investigated employment of SIL scheme on three different color semiconductor edge-emitting laser diodes *viz.* blue (450 nm), green (520 nm) and red (638 nm). In particular, we analyzed the effect of injection current, power injection ratio (ratio of the feedback and source optical power) and external cavity length on the spectral linewidth and modulation bandwidth performance of the laser diodes. We report significantly improved bandwidth of up to  $\sim 57\%$  (from 1.53 GHz to 2.41 GHz) and  $\sim 31\%$  (1.72 GHz–2.26 GHz) and narrowed linewidth of  $\sim 9$  times, using SIL blue and green laser diodes, respectively. With this report, the prospects of employing this simpler and energy efficient assisting technique (compared to the external injection locking counterpart) for improving the laser quality and achieving high bitrate optical wireless communication is compelling.

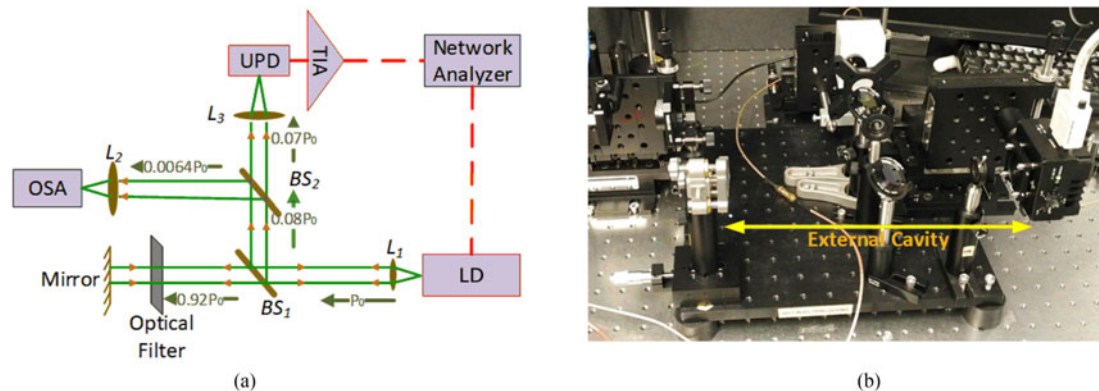


Fig. 1. (a) Block schematic of the self-injection locking experimental setup where the mirror serves as a means for optical feedback into the laser diode (LD). The green and red lines correspond to the optical and electrical path, respectively, and the orange arrows show the direction of the light propagation. The numbers shown on the beam path corresponds to the percentage of optical power flow from the beam splitters. (b) Photograph of the experimental setup showing the external cavity formation.

## 2. Experimental Setup

The schematic of the experimental setup and the corresponding laboratory photograph are shown in Fig. 1(a) and (b), respectively. We used commercially available 450 nm (Thorlabs PL450B, blue), 520 nm (Thorlabs L520P50, green), and 638 nm (Thorlabs L638P040, red) TO-can single spatial mode laser diodes as transmitter sources. The coherent transmitted light-beam from the laser diode was collimated using an aspheric lens  $L_1$  (Thorlabs A110TM-A) of focal length 6.24 mm. A 92:8% pellicle beam-splitter  $BS_1$  (Thorlabs BP107) was used to facilitate self-injection locking and performance measurement simultaneously. The 92% of the optical power was transmitted towards a silver coated mirror (Thorlabs PF10-03-P01), which forms one end of the  $\sim 26$  or  $56$  cm long external cavity. The mirror is selected to have high reflectivity of  $>97.5\%$  in the visible region to ensure strong optical feedback into the edge-emitting laser's front facet that forms the other end of the external cavity. To adjust the optical power injection ratio, a compact neutral density filter (Newport FR-CV-75) is employed in the path of the beam and inside the external cavity to control the feedback optical power. The other 8% of the optical power from  $BS_1$  was again split with an identical 92:8% beam-splitter ( $BS_2$ ), thus enabling SIL characterization. While the spectral linewidth measurements were performed via an optical spectrum analyzer (OSA, Yokogawa AQ6373B with 0.02 nm resolution) at the 8% of the optical power end, modulation bandwidth measurements were carried out via an ultra-fast photodiode UPD (Alphaslas UPD-50-UP) at the 92% of the optical power end. Since the responsivity of UPD at 450 nm ( $\sim 0.12$  A/W), 520 nm ( $\sim 0.25$  A/W), and 638 nm ( $\sim 0.5$  A/W) was weak, a 26 dB linear trans-impedance amplifier TIA (Tektronix PSPL5865) was incorporated in the system after the UPD to amplify the received electrical signal before sending to 67 GHz Network Analyzer (Agilent E8361C) to observe the frequency response. The distance between  $L_1$  and UPD forms the free-space channel link that is measured to be  $\sim 18$  cm. Since, it was very difficult to measure the optical power at the laser front facet owing to the space limitation, the total integrated optical power of the laser was measured after  $L_1$  using a calibrated Si photodetector (Newport 818-SL) and then the feedback power was calculated considering entire losses due to external cavity length, beam-splitter, and mirror, at the laser front-facet (before  $L_1$ ). Hence, the optical power injection ratio ' $R$ ' is estimated at  $L_1$  as the ratio of these two power values.

## 3. Results and Discussion

In our experimental setup, we installed each color TO-can laser one after the other as shown in Fig. 1(a) and performed a thorough investigation of self-injection locking. All the measurements

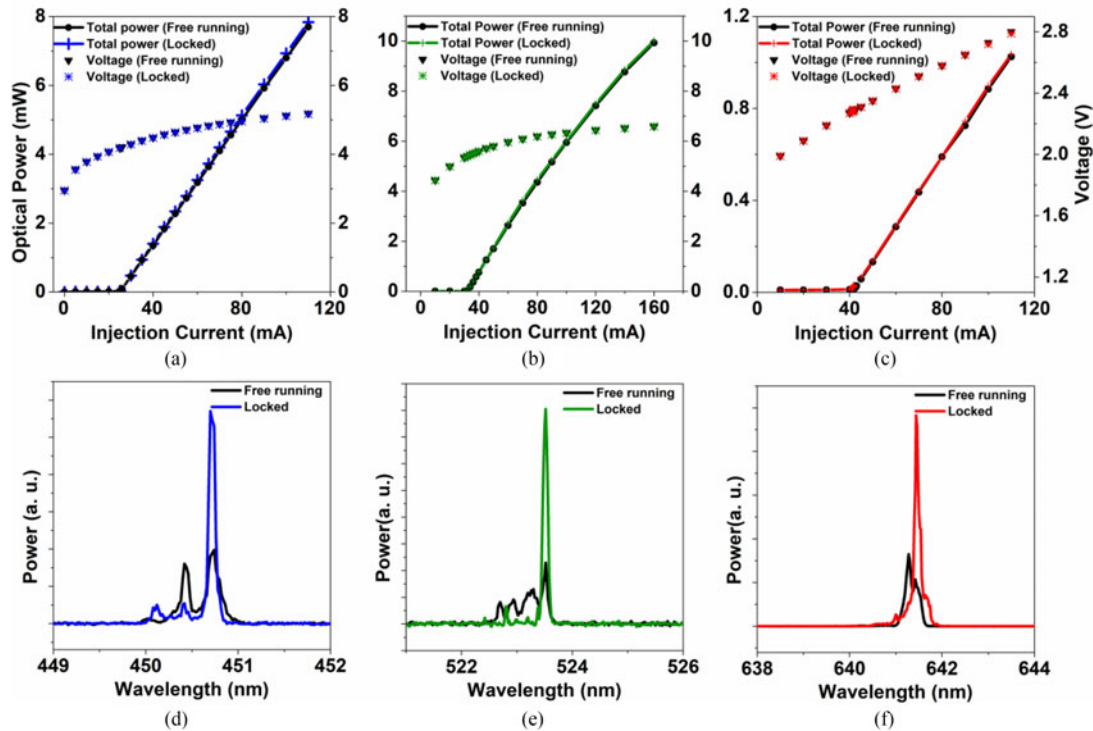


Fig. 2. Comparison of the light optical power (from front facet) and voltage characteristics of (a) blue (b) green and (c) red laser diode versus the continuous wave injection current, under the free-running (black color) and self-injection locked (colored) cases. The corresponding lasing spectrum under free-running (black color) and self-injected locked (colored) case for (d) blue (e) green and (f) red laser diodes.

were taken at fixed room temperature (20 °C) via a temperature controlled built-in heat sink of the laser mount (Thorlabs LDM9T).

### 3.1 L-I-V and Spectral Characteristics of Self-Injection Locked Visible Lasers

Fig. 2(a)–(c) illustrates the front facet total optical power (integrated) and voltage characteristics versus the injection current ( $L - I - V$ ) for the blue (450 nm), green (520 nm), and red (638 nm) (BGR) color semiconductor laser diodes under free-running and self-injection locked states, for an external cavity length of 26 cm in the latter case. The threshold current ( $I_{th}$ ) of the laser diodes in the free-running case are found to be 25.8 mA, 34 mA, and 42.7 mA, while in self-injection locked case, they are found to reduce to 25.4 mA, 33.7 mA, 41.9 mA. This reduction in the threshold current is considered as a key signature of successful locking and has been previously observed in [19], [20]. This phenomenon has been attributed to the change in the gain threshold due to the difference in the localized refractive index in the active region of the laser diode [21]. The new gain,  $g_c$ , required for the laser to turn-on can be significantly smaller from the free-running threshold gain,  $g_{th}$ , depending on the optical power injection ratio ( $R$ ) and the phase of the optical feedback,  $\phi_{ext}$ , as described in Eqn. (1) below:

$$g_c = g_{th} - \frac{|C| (2\sqrt{R})}{L} \cos(\phi_{ext}) \quad (1)$$

where,  $C$  is the coupling efficiency that depends on the reflectivity of the front laser facet from where the feedback optical power is re-injected. Hence, under phase matching condition ( $\phi_{ext} = 0^\circ$ ) of the optical feedback (which we accomplished by fine tuning of the external laser cavity length),  $g_c$  is

expected to decrease, thus reducing the threshold current in the locked case. Moreover, a particular Fabry-Perot mode is locked when it is sustainable in both the cavities i.e., laser and external cavity since this configuration form a coupled cavity system [19]. FP mode spacing of the external cavity, which is calculated from Eqn. (2):

$$\Delta\lambda = \frac{\lambda_c^2}{2nL_{ext}} \quad (2)$$

is found to be  $\sim 0.4$  pm ( $\lambda_c = 450$  nm for blue),  $\sim 0.5$  pm (523 nm for green), and  $\sim 0.8$  pm (and 641 nm for red) for a cavity length,  $L_{ext} \approx 26$  cm and refractive index,  $n = 1$  (free space), is approximately three orders of magnitude smaller than the laser cavity mode spacing of  $\sim 0.3$  nm (blue),  $\sim 0.25$  nm (green), and  $\sim 0.15$  nm (red), that are obtained from the corresponding free-running lasing spectrums (Fig. 2(d)–(f)). Hence, the wavelength of locked FP modes is essentially dictated by the laser cavity mode spacing that is expected to vary due to the localized refractive index of the active region [22]. It is noteworthy to mention here that fine tuning (micrometer range) of the external cavity is essential to match the phase of the optical feedback power of a particular FP mode for it to be injection locked, else mode hopping would occur as previously reported [20]. After careful tuning of the external cavity, a stable, single locked FP mode was observed in blue, green, and red (BGR) laser diodes, which are shown in Fig. 2(d)–(f), respectively. The free-running spectrum of the laser diodes is also plotted in the same figure for comparison purpose. The peak powers of locked FP modes are found to increase considerably, thanks to suppression of the side modes (improved side-mode-suppression-ratio, SMSR) which enabled consolidation of the energies from the side modes into the single dominant longitudinal mode. This subsequently reduced the spectral linewidth (measured at the full-width-at-half-maximum, FWHM, considering the whole lasing spectrum) of the self-injection locked lasers.

### 3.2 Stability of Self-Injection Locked Laser Diodes

A stability test is initially performed on the self-injection locked laser diodes at a fixed injection current to ascertain steady operation of this assisting scheme in the visible region. Fig. 3(a)–(f) depicts the variation in total (integrated) optical power, peak power, peak wavelength, and SMSR of the self-injection locked mode of the BGR lasers along with the free-running counterpart, over a span of 20 minutes with 2 minutes interval. The injection currents for the blue, green, and red lasers are selected to be 54 mA, 120 mA, and 102 mA, respectively. In general, the stability of total power and peak power of the locked BGR laser diodes (Fig. 3 (a)–(c)) are found to be with comparable to the free-running case or better, particularly for the red laser. Moreover, in all the cases, the self-locked power (total and peak) was found to be higher than the free-running case, a signature of injection locking which has been discussed comprehensively in the earlier section. Referring to Fig. 3 (d)–(f), which plots the variation of peak locked mode wavelength and SMSR, again exhibited similar or superior performance from the injection-locked lasers compared to free-running case and across the entire time span, mainly for green and red lasers. Note that a remarkable achievement of  $\sim 20$  dB SMSR is measured from self-injection locked blue laser, which, to the authors' knowledge, is one of the best values ever reported [23]. Comparable total power and the peak power values of this laser diode suggests close to single mode operation. Alternatively, green and red laser diodes exhibited SMSR values of  $\sim 6$  and  $\sim 8$  dB, respectively. In general, utilizing self-injection locking scheme on BGR laser diodes improved the performance characteristics while preserving their stability with time, which is crucial for deployment in optical communications.

### 3.3 Effect of Injection Current

Next, self-injection locking characteristics of the BGR laser diodes are investigated at different injection currents. Fig. 4(a)–(c) compares the spectral linewidths of self-locked and free-running states of the lasers at different above-threshold injection currents. In general, the spectral linewidth is found to decrease noticeably in the locked case and found to be independent of the injection current,

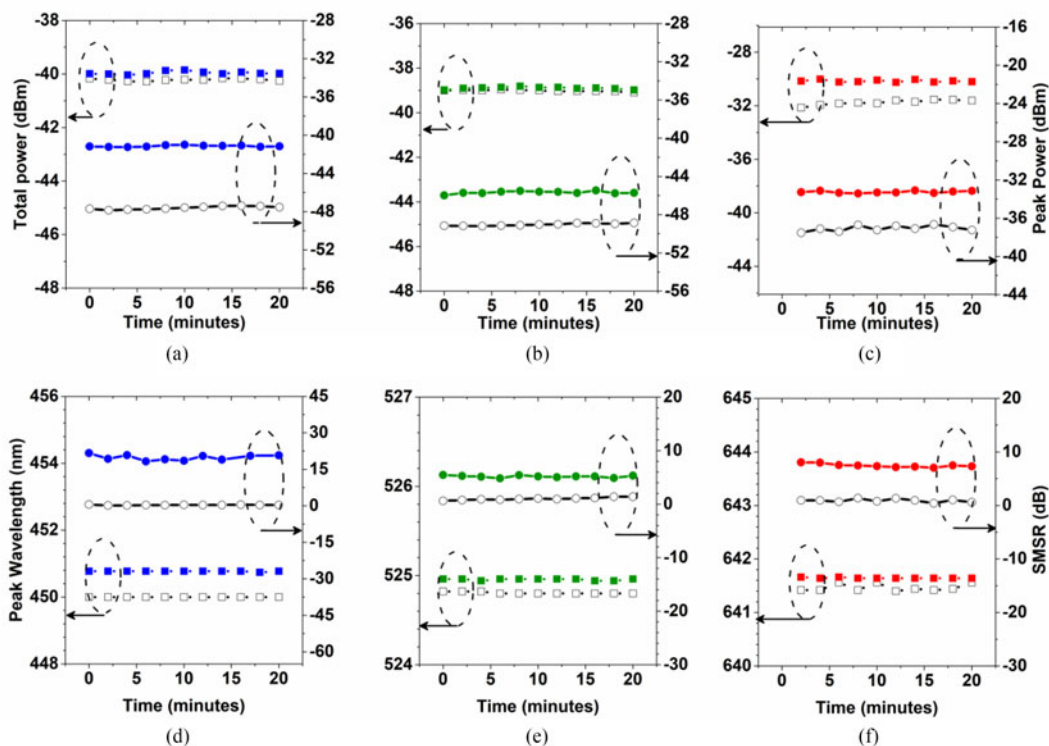


Fig. 3. Stability analysis of (a) and (d) blue, (b) and (e) green, and (c) and (f) red self-injection locked laser diodes, showing the variation in total integrated power (left vertical-axis) and peak power (right vertical axis) (a, b, c); and peak wavelength (left vertical-axis) and SMSR (right vertical axis) (d, e, f) within time span of 20 minutes at 2 minutes interval. The free-running (black open symbols) results are also shown for comparison purpose. The measurements were obtained at fixed 54 mA, 120 mA, and 102 mA injection current for blue (blue closed symbols), green (green closed symbols), and red (red closed symbols) laser diodes, respectively.

particularly in green and red laser diodes, which is attributed to the effective self-injection locking. For the blue laser diode, a reduction in the spectral linewidth of  $<0.2$  nm is measured in the injection current range of 40–90 mA with a narrow value of  $<0.13$  nm at  $\leq 80$  mA, which corresponds to  $\sim 5$ – $8$  times linewidth reduction. However, for  $>90$  mA a degradation in the spectral linewidth is observed and ascribed, in part, to the deteriorating laser performance, quantum efficiency in particular, at high injections. On the other hand, self-locked FP mode linewidths with increasing injection current are found to be uniform for green laser diode, exhibiting an average value of  $\sim 0.17$  nm in the entire range (40–160 mA) and attaining a maximum linewidth reduction of  $\sim 9$  times at 100 mA (0.1 nm in free-running vs 0.11 nm under injection locked). The scope of performance improvement of red laser diode via SIL was found to be least among the examined three visible laser diodes, with a measured  $\sim 0.23$  nm spectral linewidth at 110 mA injection current under locked case compared to  $\sim 0.38$  nm under free-running state, as illustrated in Fig. 4(c). We postulate that a close to single mode free-running operation at almost every injection current might be the reason behind this minute enhancement owing to the high-quality and mature InGaP/AlGaInP active region design and growth technology. It is to be noted that the spectral linewidth of the laser diodes is measured at FWHM in both self-injection locked and free-running scenario due to the observation of single (multiple) self-injection locked mode operation at lower (higher) injection currents. Moreover, the injection current range of all the laser diodes are selected in the linear  $L - I - V$  regime operation, and hence the estimated power injection ratio 'R' is assumed to be independent of current attaining values  $\sim -1.3$ ,  $\sim -3.0$  and  $\sim -2.2$  dB, respectively, for BGR laser diodes.

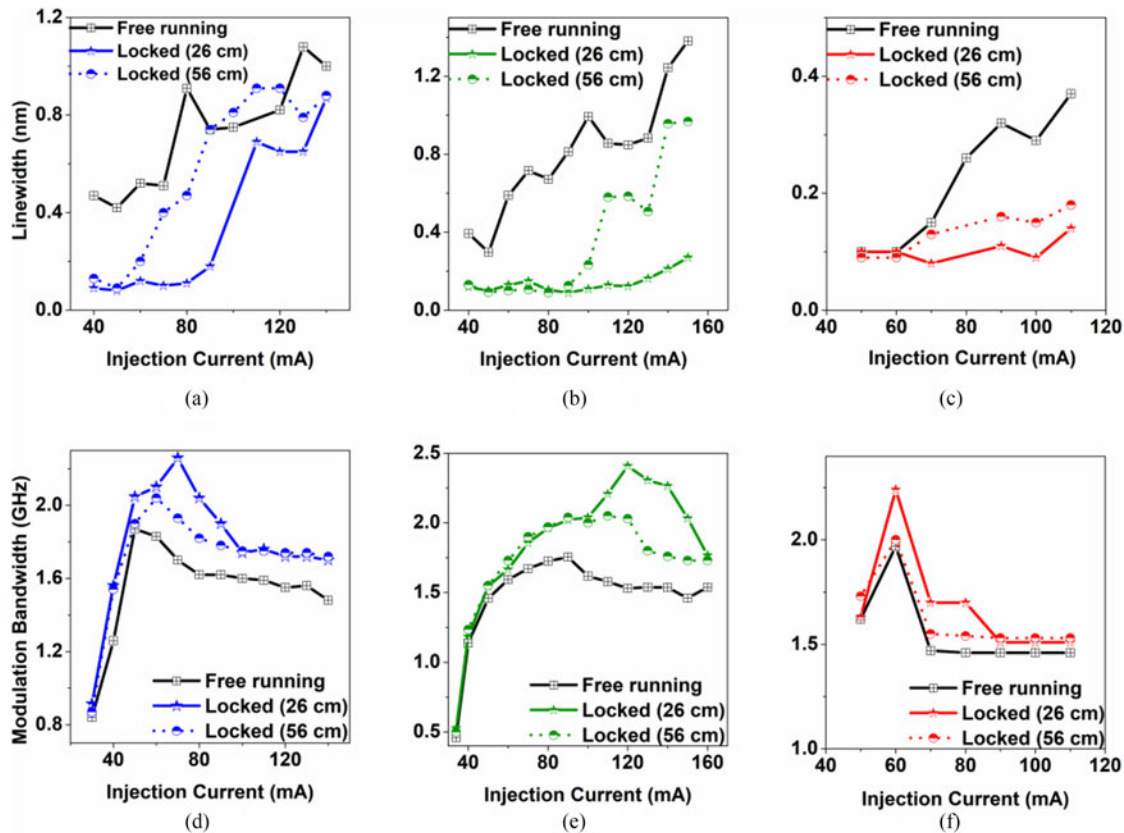


Fig. 4. Variation of the spectral linewidth (top row) and modulation bandwidth (bottom row) as a function of injection current for blue (a) and (d), green (b) and (e), and red (c) and (f) laser diodes. The results of free-running (black color) are also plotted alongside self-injection locked counterpart (colored) in each case. The injection currents (injection ratios,  $R$ ) for blue, green, and red laser diode are fixed at 50 ( $-1.3$ ), 40 ( $-3.0$ ), and 100 ( $-2.2$ ) mA (dB), respectively.

Next, small-signal modulation response of the BGR laser diodes has been performed to identify their transmission capabilities under direct modulation technique. Fig. 4(d)–(f) plots the measured  $-3$  dB modulation bandwidth results for the free-running and self-locked scenarios and under different injection currents. For blue and green laser diodes, a similar bandwidth variation trend is observed with trivial improvement at low and high injection currents i.e.,  $\leq 2.0I_{th}$  and  $\geq 4.0I_{th}$ , while a considerable bandwidth enhancement is noticed at medium injection currents. Moreover, the curves follow a typical laser frequency response behavior with superior bandwidth values at medium injection and then deteriorating performance at lower and higher injection currents [24]. A maximum of  $\sim 1.31$  times ( $\sim 31\%$ ) and  $\sim 1.57$  times ( $\sim 57\%$ ) improvement in the modulation bandwidth is observed from self-injection locked blue (green) laser diodes at 70 (120) mA injection current, as depicted in Fig. 4(d) and (e), respectively. Thus, an improvement of  $\sim 540$  and  $\sim 880$  MHz is attained with self-injection locked blue and green laser with measured bandwidth values of 2.26 (1.7 GHz under free-running) and 2.41 GHz (1.53 GHz under free-running) on blue and green lasers, respectively. On the other hand, red laser diode showed  $\sim 270$  MHz ( $\sim 14\%$ ) improvement in the modulation bandwidth at 60 mA and displayed a similar trend of the bandwidth performance curve, as shown in Fig. 4(f). Hence, these results show the effectiveness of self-injection locking technique in substantially improving the laser dynamic performance characteristics and potentially extending the laser modulation capability, thus, contributing towards the achievement of high bit-rate visible optical wireless communication.



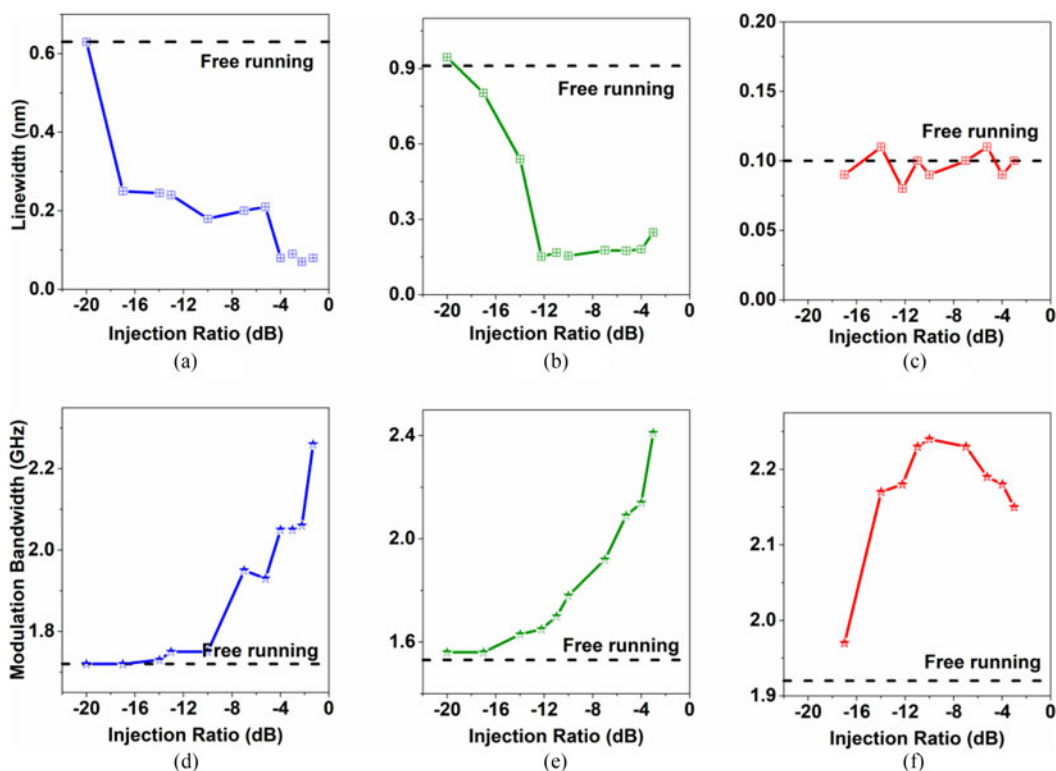


Fig. 5. Variation of the spectral linewidth (top row) and modulation bandwidth (bottom row) as a function of injection ratio for blue (a) & (d), green (b) & (e), and red (c) & (f) laser diodes. The results of free-running (black color) are also plotted alongside self-injected counterpart (colored) in each case. The injection current for blue, green, and red laser diodes are fixed at 70, 120, and 60 mA, respectively.

### 3.4 Effect of Optical Power Injection Ratio

Optical power injection ratio ‘ $R$ ’ plays an important role in the self-injection locked laser dynamics. It is directly proportional to the spectral linewidth reduction and the mode stability when the round trip phase of the feedback power is zero [21]. It has been shown that bi-stability or multi-stability (i.e., dual or multiple locked modes) might occur with an inverse phase at the optical feedback. To demonstrate the impact of  $R$  on the linewidth and modulation bandwidth of the self-injection locked laser diodes, we fixed the injection current and employed an optical filter to control the feedback power to be re-injected into the laser front facet. The results of blue and green laser diodes, which are illustrated in Fig. 5(a) and (b), depicts a significant linewidth reduction with increasing injection ratio and later saturate in higher value. Thanks to an increase in the peak power of the locked mode with increasing injection ratio (via higher optical feedback power), which dictated this performance improvement. However, this behavior is not observed in the self-injection locked red laser diode, as illustrated in Fig. 5(c), and an average spectral linewidth of  $\sim 0.1$  nm is measured at all injection ratios, which is similar in value to that of the free-running case. It is worth mentioning here that two separate experimental results that are plotted in Fig. 4(c) and 5(c) demonstrate an analogous measured value of spectral linewidth at  $R = \sim -2.2$  dB and injection current of 60 mA, and does not show any significant improvement with  $R$ , thus further affirming the consistency of our analysis. Besides, observation of Fig. 5(a) and (b) suggests two regions of operation for blue and green lasers: linewidth reduction region (when  $-20$  dB  $\leq R \leq -4$  dB for blue and  $-20$  dB  $\leq R \leq -12.2$  dB for green laser diodes) and linewidth saturation region (when  $R > -4$  dB for blue and  $R > -12.22$  dB for green laser diodes). Increasing  $R$  improves the locking efficiency by matching the feedback phase of locked mode, and later saturates, indicating possible transition approach into

an unstable region of locking operation for  $R > -1.3$  dB (blue) and  $R > -4$  dB (green), as has been comprehensively studied and observed on different color laser diodes [22], [25]. Injection locked red laser diode, on the other hand, does not exhibit such behavior owing to 60 mA injection current operation, as discussed above. A proper choice of injection current, such as 80 mA, would potentially enable observation of both the linewidth regions with increasing  $R$  in the self-locked red laser diode. Nevertheless, a maximum improvement in the spectral linewidth by  $\sim 9$  times for blue,  $\sim 6$  times for green, and  $\sim 1.2$  times for red color laser diodes are achieved; corresponding to  $\sim 0.07$  nm,  $\sim 0.15$  nm and  $\sim 0.08$  nm locked measured linewidth values at  $R = \sim -2.2$  dB,  $\sim -12.2$  dB, and  $\sim -12.2$  dB, respectively.

The effect of power injection ratio on the modulation bandwidth is also measured and are plotted in Fig. 5(d)–(f) for the BGR lasers, respectively. As expected, increasing  $R$  substantially enhances the modulation bandwidth in all the three color laser diodes under self-injection locking. Thanks to the increased feedback power into the laser active region and the reduction in the laser intensity noise [26], thereby effectively improving the locking efficiency up to  $R \leq -1.3$  dB,  $\leq -3.0$  dB and  $\leq -10$  dB for BGR laser diodes, respectively. In this case, saturation region of operation is not observed in all the three lasers and instead, an apparent modulation bandwidth degradation region is observed in the red laser for  $R > -10$  dB. This again is a possible signature of transition of locking operation to an unstable region. Increasing  $R$  further beyond  $\sim -1.3$  and  $\sim -3.0$  dB in blue and green laser diodes might allow observation of this region. It is to be noted that these are estimated  $R$  values and hence we expect a variation with the actual values. However, due to the limitation of the experimental set up this region could not be investigated. In summary, a maximum bandwidth enhancement of  $\sim 880$  MHz (1.53–2.41 GHz) for green,  $\sim 540$  MHz (1.72–2.26 GHz) for the blue and  $\sim 320$  MHz (1.92–2.24 GHz) for the red laser diodes are achieved via self-injection locking technique. It is worth mentioning at this instance that all these lasers exhibited significant performance improvement compared to our first and initial results on spectral linewidth ( $\sim 1.3$  times) and modulation bandwidth ( $\sim 2$  times) improvement, which were reported on an unoptimized setup [16], [17].

### 3.5 Effect of External Cavity Length

In this section, the effect of external cavity length on the performance of self-injection locked BGR laser diodes is studied. The results of changing  $L_{ext}$  from 26 cm to 56 cm on the spectral linewidth and the modulation bandwidth is compared in Fig. 4 (a)–(c) and (d)–(f), respectively. At higher injection current, the performance of the longer external cavity (56 cm) is found to degrade faster than the shorter cavity and reaches close to the free-running case. For instance, the spectral linewidth of the longer cavity starts to degrade at an early injection current of 60 (100) mA compared to the shorter cavity length that showed performance degradation from 80 (120) mA for the blue (green) laser diodes. On the other hand, red laser diode showed performance degradation from a similar current value of 70 mA from both the cavity lengths. This is attributed to the inferior estimated  $R$  value of the longer cavity system due to an additional path and scattering losses compared to the shorter cavity length, and are estimated to be  $-1.6$ ,  $-4.0$  and  $-3.0$  dB. Hence, a poorer performance from the longer cavity is obvious and is in good agreement with the results elucidated in the previous section. As expected, the modulation bandwidth at longer cavity length also exhibited performance degradation in self-injection locked BGR lasers, and attain values as tabulated in Table. 1 and compared to 26 cm cavity length results at fixed injection currents. In summary, as depicted in Fig. 4, a maximum improvement of the modulation bandwidth of 240 MHz (1.48 GHz to 1.72 GHz at 140 mA) and  $\sim 4.6$  times (0.42 nm to 0.09 nm at 50 mA) reduction in the linewidth for blue,  $\sim 500$  MHz (1.53 GHz to 2.03 GHz at 120 mA) and  $\sim 7.4$  times (0.67 nm to 0.09 nm at 80 mA) for green, and 80 MHz (1.47 GHz to 1.55 GHz at 70 mA) and  $\sim 2$  times (0.37 nm to 0.18 nm 100 mA) for red laser diode is measured from the 56 cm cavity length. In general, the performance of self-injection locking in an external cavity is found to be dictated primarily by the variation in the power injection ratio due to the cavity length.

TABLE 1  
Performance Comparison of 26 and 56 cm External Cavity Lengths on Self-Injection Locked BGR Laser Diodes at Fixed Injection Currents.

External cavity length		26 cm		56 cm	
Blue	Injection ratio (dB)	-1.3		-1.6	
	Injection current (mA)	70	80	70	80
	Spectral linewidth (nm)	0.1	<b>0.11*</b>	0.4	0.47
	Modulation bandwidth (~GHz)	<b>2.26</b>	2.04	1.93	1.82
Green	Injection ratio (dB)	-3.0		-4.0	
	Injection current (mA)	100	120	100	120
	Spectral linewidth (nm)	<b>0.11</b>	0.12	0.23	0.59
	Modulation bandwidth (GHz)	2.04	<b>2.41</b>	2	2.03
Red	Injection ratio (dB)	-2.2		-3.0	
	Injection current (mA)	60	100	60	100
	Spectral linewidth (nm)	0.09	<b>0.09</b>	0.09	0.15
	Modulation bandwidth (GHz)	<b>2.24</b>	1.53	2	1.53

\* Bold numbers correspond to the measured values at which maximum improvement in spectral linewidth and modulation bandwidth were achieved from 26 cm cavity.

#### 4. Conclusion

A self-injection locked scheme is proposed and comprehensively investigated to improve the dynamic performance of visible laser diodes and hence their modulation capability. This simple and cost-effective assisting scheme is implemented on InGaN/GaN blue and green, and InGaP/AlGaInP red laser diodes and systematically studied the effect of injection current, optical power injection ratio and external cavity length, on the spectral linewidth and modulation bandwidth of these laser diodes. A maximum improvement of 880 MHz (~57%) and 540 MHz (~31%) in bandwidth and ~9 times reduction in linewidth of self-injection locked blue and green lasers are, respectively, measured, compared to their free-running counterpart. Through this simple, robust, energy efficient and cost-effective scheme, the performance of the laser-based visible light transmitters could be significantly improved, thus a viable platform to achieve future high data rate visible and underwater optical wireless light communication.

#### References

- [1] Cisco Public, "Cisco visual networking index: forecast and methodology, 2016-2021," 2017. [Online]. Available: <https://www.cisco.com/c/en/us/solutions/collateral/service-provider/visual-networking-index-vni/complete-white-paper-c11-481360.pdf>
- [2] A. M. Khalid, G. Cossu, R. Corsini, P. Choudhury, and E. Ciaramella, "1-Gb/s transmission over a phosphorescent white LED by using rate-adaptive discrete multitone modulation," *IEEE Photon. J.*, vol. 4, no. 5, pp. 1465–1473, Oct. 2012.
- [3] C. Kottke, J. Hilt, K. Habel, J. Vučić, and K.-D. Langer, "1.25 Gbit/s visible light WDM link based on DMT modulation of a single RGB LED luminary," in *Proc. Eur. Conf. Exhib. Opt. Commun.*, 2012, paper We.3.B.4.
- [4] C. Lee *et al.*, "2 Gbit/s data transmission from an unfiltered laser-based phosphor-converted white lighting communication system," *Opt. Exp.*, vol. 23, no. 23, pp. 29779–29787, 2015.
- [5] B. Janjua *et al.*, "Going beyond 4 Gbps data rate by employing RGB laser diodes for visible light communication," *Opt. Exp.*, vol. 23, no. 14, pp. 18746–18753, 2015.
- [6] Y. Huang, Y. Chi, H. Kao, C. Tsai, and H. Wang, "Blue laser diode based free-space optical data transmission elevated to 18 Gbps over 16 m," *Sci. Rep.*, vol. 7, 2017, Art. no. 10478.
- [7] Y. Chi *et al.*, "Phosphorous diffuser diverged blue laser diode for indoor lighting and communication," *Sci. Rep.*, vol. 5, no. 1, Nov. 2016, Art. no. 18690.
- [8] J. Retamal *et al.*, "4-Gbit/s visible light communication link based on 16-QAM OFDM transmission over remote phosphor-film converted white light by using blue laser diode," *Opt. Exp.*, vol. 23, no. 26, pp. 33656–33666, Dec. 2015.
- [9] C.-L. Ying, H.-H. Lu, C.-Y. Li, C.-J. Cheng, P.-C. Peng, and W.-J. Ho, "20-Gbps optical LiFi transport system," *Opt. Lett.*, vol. 40, no. 14, pp. 3276–3279, 2015.
- [10] S. Viola, M. S. Slim, S. Watson, S. Videv, H. Haas, and A. E. Kelly, "15 Gb/s OFDM-based VLC using direct modulation of 450 GaN laser diode," in *Advanced Free-Space Optical Communication Techniques and Applications III*, vol. 10437, 2017, Art. no. 104370E.

- [11] M. T. A. Khan, E. Alkhazraji, A. Ragheb, H. Fathallah, and M. Z. M. Khan, "Far L-band single channel high speed downstream transmission using injection-locked quantum-dash laser for WDM-PON," in *Proc. 5th Int. Conf. Photon., Opt. Laser Technol.*, 2017, pp. 90–94.
- [12] M. Shemis *et al.*, "Broadly tunable self-injection locked InAs/InP quantum-dash laser based fiber/FSO/hybrid fiber-FSO communication at 1610 nm," *IEEE Photon. J.*, vol. 10, no. 2, Apr. 2018, Art. no. 7902210.
- [13] X.-Y. Lin *et al.*, "A 56-Gbps PAM4 LiFi transmission system based on VCSEL with two-stage injection-locked technique," in *Proc. Opt. Fiber Commun. Conf.*, 2017, paper W2A.37.
- [14] W.-S. Tsai *et al.*, "A 50 m/40 Gbps 680-nm VCSEL-based FSO communication," in *Proc. IEEE Photon. Conf.*, 2016, pp. 39–40.
- [15] H.-H. Lu *et al.*, "An 8 m/9.6 Gbps underwater wireless optical communication system," *IEEE Photon. J.*, vol. 8, no. 5, Oct. 2016, Art. no. 7906107.
- [16] M. Shamim *et al.*, "High performance self-injection locked 524 nm green laser diode for high bitrate visible light communications," in *Proc. Opt. Fiber Commun. Conf.*, 2018, paper Th2A.15.
- [17] M. Shamim *et al.*, "Enhanced performance of 450 nm GaN laser diodes with an optical feedback for high bit-rate visible light communication," in *Proc. Conf. Lasers Electro-Opt.*, 2018, paper JTu2A.29.
- [18] P. S. Donvankar, A. Savchenkov, and A. Matsko, "Self-injection locked blue laser," *J. Opt.*, vol. 20, no. 4, Apr. 2018, Art. no. 45801.
- [19] W. Liang *et al.*, "Ultralow noise miniature external cavity semiconductor laser," *Nature Commun.*, vol. 6, 2015, Art. no. 7371.
- [20] D. M. Kane and K. A. Shore, *Unlocking Dynamical Diversity: Optical Feedback Effects on Semiconductor Lasers*, vol. 1. Hoboken, NJ, USA: Wiley, 2005, p. 356.
- [21] K. Petermann, "External optical feedback phenomena in semiconductor lasers," *IEEE J. Sel. Topics Quantum Electron.*, vol. 1, no. 2, pp. 480–489, Jun. 1995.
- [22] L. A. Coldren, S. W. Corzine, and M. L. Mashanovitch, *Diode Lasers and Photonic Integrated Circuits*. 2012.
- [23] M. Chi, O. B. Jensen, and P. M. Petersen, "Tuning range and output power optimization of an external-cavity GaN diode laser at 455 nm," *Appl. Opt.*, vol. 55, no. 9, pp. 2263–2269, 2016.
- [24] S. Watson *et al.*, "High speed visible light communication using blue GaN laser diodes," *Proc. SPIE*, vol. 9991, 2016, Art. no. 99910A.
- [25] J. Ohtsubo, *Semiconductor Lasers, Stability, Instability, and Chaos*. Heidelberg, Germany: Springer, 2008.
- [26] H. Simos, A. Bogris, D. Syvridis, and W. Elsasser, "Intensity noise properties of mid-infrared injection locked quantum cascade lasers: I. Modeling," *IEEE J. Quantum Electron.*, vol. 50, no. 2, pp. 98–105, Feb. 2014.